2014

Fluid-Structure Interaction of a Reed Type Valve Subjected to Piston Displacement

Olga Estruch
Heat and Mass Transfer Technological Center – Polytechnic University of Catalonia, Terrassa (Barcelona), Spain, olga@cttc.upc.edu

Oriol Lehmkuhl
oriol@cttc.upc.edu

Joaquim Rigola
Heat and Mass Transfer Technological Center – Polytechnic University of Catalonia, Terrassa (Barcelona), Spain, quim@cttc.upc.edu

Carles David Pérez-Segarra
Heat and Mass Transfer Technological Center – Polytechnic University of Catalonia, Terrassa (Barcelona), Spain, segarra@cttc.upc.edu

Fluid-Structure Interaction of a Reed Type Valve Subjected to Piston Displacement

Olga ESTRUCH[1*], Oriol LEHMKUHL[1,2], Joaquim RIGOLA[1], Carles-David PÉREZ SEGARRA[1]

[1] Heat and Mass Transfer Technological Center (CTTC), Universitat Politècnica de Catalunya (UPC), Barcelona, Spain
cttc@cttc.upc.edu, http://www.cttc.upc.edu/

[2] Termo Fluids S.L.
Barcelona, Spain
+34-93-783.61.13, termofluids@termofluids.com, http://www.termofluids.com

* Corresponding Author

ABSTRACT

The present paper deals with the dynamic simulation of the fluid flow through reed valves and is concerned with a partitioned fluid-structure interaction coupling scheme. In this work attends the newly in-house implemented computational fluid dynamics (CFD) and moving mesh coupled code TermoFluids. The CFD solver consists of a three-dimensional explicit finite volume fractional-step algorithm formulated in a second-order, conservative and collocated unstructured grid arrangement. Large eddy simulation is performed to solve the turbulent flow, using the subgrid scale WALE model. A radial basis function interpolation procedure is used to dynamically move the mesh according with the displacement of the valve. A simplified geometry of an axial hole plus a rectangular diffuser with a piston based inlet condition is considered. The valve dynamics is modelled by means of the normal mode summation methodology and a coefficient of restitution is applied to model the impact between the valve and its seat. A parametric study is presented in order to analyze the influence of the valve thickness.

1. INTRODUCTION

Fluid-structure interactions (FSI) arise when the motion of a structure is instigated by a fluid flow and viceversa, the flow field behaviour is affected by the movement or deformation of the structure. This type of coupling can be encountered in a great amount of industrial applications, such as the design of aircrafts, the study of aerolastic instabilities of bridges and buildings, the optimisation of wind turbines or in bio-fluid mechanics research like heart valve development, among others. In those cases, the understanding of the fluid flow behaviour or the awareness of the dynamic action of the structure can be essential to improve engineering designs and optimisations. Therefore, accompanied by a great enhance in computational resources, in the last years the numerical simulation has become an important tool to predict FSI applications.

In the field of reciprocating compressors, the developing of reed type valves is a challenging task. The understanding of the fluid flow behaviour through the valve reed is essential to improve the valve design. Hence, the present study attempts the dynamic simulation of this fluid-structure interaction (FSI) problem, taking into account valve movement due to piston displacement.

In this work attends the in-house implemented CFD and moving mesh coupled code TermoFluids (Lehmkuhl et al. (2009)). The CFD solver consists of a three-dimensional explicit finite volume fractional-step algorithm formulated in a second-order, conservative and collocated unstructured grid arrangement. Large-eddy simulation is used to model the turbulent flow by means of the subgrid scale WALE model (Nicoud and Ducros (1999)). The pressure equation is solved through a conjugate gradient solver with Jacobian preconditioning. Referring to the moving mesh procedure, a radial basis function (RBF) interpolation strategy is used, which allows the dynamic deformation of the mesh according to the displacement of the valve (Boer et al. (2007); Jakobsson and Amoignon (2007); Estruch et al. (2012, 2013)). The CFD and moving mesh coupling is built by the space conservation law (SCL) (Orozco (2006); Breuer et al. (2012)).

The newly implemented FSI global solver is based on a partitioned coupled algorithm in which the dynamic action of the valve is modelled by the reed vibration theory by means of the normal mode summation method (Soedel (1992)). This methodology assumes that the valve motion results from the superposition of the valve vibration modes, which are evaluated based on the modal behaviour of uniform cantilever beams (Young and Felgar (1949)). Similarly, Sheu and Hu (2000); Ooi et al. (1992) applied the assumed-modes methodology to simulate the dynamic behaviour of reed valves but using polynomial shape functions instead of normal modes shape functions. In contrast to conventional computational structural dynamics (CSD) solvers, this alternative performs a fast transient prediction of the valve displacement and, without losing reliability on the solid dynamics, this allows to focus on the fluid flow behaviour study.

As a preliminary approach, a simplified geometry of an axial hole plus a rectangular diffuser with a piston based inlet condition is considered. The valve impact against its seat is taken into account; therefore, a coefficient of restitution is advocated to the velocities of the valve. An immersed body procedure is used to simulate solid parts inside the domain and, particularly, to reproduce the bottom and inlet boundaries. A parametric study is carried out in order to analyse the influence of the valve thickness.

2. COMPUTATIONAL FLUID DYNAMICS

2.1 Governing equations and numerical algorithm

In the fluid domain the governing equations correspond with the incompressible Navier-Stokes and continuity equations coupled with dynamic mesh, which can be written as

$$M\left(\mathbf{u}-\mathbf{u}_g\right) = \mathbf{0} \tag{1}$$

$$\frac{\partial \mathbf{u}}{\partial t} + C\left(\mathbf{u}-\mathbf{u}_g\right)\mathbf{u} + \nu D\mathbf{u} + \rho^{-1}G\mathbf{p} = \mathbf{0} \tag{2}$$

where $\mathbf{u} \in \mathbb{R}^{3m}$ and $\mathbf{p} \in \mathbb{R}^{m}$, being m the total number of control volumes (CV) of the discretized domain. Convective and diffusive operators in the momentum equation for the velocity field are given by $C(\mathbf{u}) = (\mathbf{u} \cdot \nabla) \in \mathbb{R}^{3m\times 3m}$, $D = -\nabla^2 \in \mathbb{R}^{3m\times 3m}$ respectively. Gradient and divergence (of a vector) operators are given by $G = \nabla \in \mathbb{R}^{3m\times m}$ and $M = \nabla\cdot \in \mathbb{R}^{m\times 3m}$ respectively.

The governing equations have been discretized on a collocated unstructured grid arrangement by means of second-order spectro-consistent schemes (see Verstappen and Veldman (2003)). Such schemes are conservative, *i.e.* they preserve the kinetic energy equation. These conservation properties are held if, and only if the discrete convective operator is skew-symmetric ($C_c(\mathbf{u}_c) = -C_c^*(\mathbf{u})$), the negative conjugate transpose of the discrete gradient operator is exactly equal to the divergence operator ($-(\Omega_c G_c)^* = M_c$) and the diffusive operator D_c, is symmetric and positive-definite (the subscript c holds for the cell-centred discretization). These properties ensure both, stability and conservation of the kinetic-energy balance even at high Reynolds numbers and with coarse grids.

For the temporal discretization of the momentum equation (Eq. 2) a fully explicit second-order self-adaptive scheme (Trias and Lehmkuhl (2011)) has been used for the convective and diffusive terms, while for the pressure gradient term an implicit first-order scheme has been used.

The velocity-pressure coupling has been solved by means of a classical fractional step projection method,

$$\mathbf{u}_c^p = \mathbf{u}_c^{n+1} + G\tilde{\mathbf{p}}_c \tag{3}$$

where $\tilde{\mathbf{p}}_c = \mathbf{p}_c^{n+1}\Delta t^n/\rho$ is the pseudo-pressure, $\mathbf{u}_c^p$ the predicted velocity, $n+1$ is the instant where the temporal variables are calculated, and Δt^n is the current time step ($\Delta t^n = t^{n+1} - t^n$). Taking the divergence of Eq. 3 and applying the incompressibility condition yields a discrete Poisson equation for $\tilde{\mathbf{p}}_c$: $L_c\tilde{\mathbf{p}}_c = M_c\mathbf{u}_c^p$. The discrete laplacian operator $L_c \in \mathbb{R}^{m\times m}$ is, by construction, a symmetric positive definite matrix ($L_c \equiv M\Omega^{-1}M^*$). Finally the mass-conserving velocity at the faces ($M_s\mathbf{u}_s^{n+1} = 0$) is obtained from the correction,

$$\mathbf{u}_s^{n+1} = \mathbf{u}_s^p - G_s\tilde{\mathbf{p}}_c \tag{4}$$

where G_s represents the discrete gradient operator at the CV faces. This approximation allows to conserve mass at the faces but it has several implications. If the conservative term is computed using $\mathbf{u}_s^{n+1}$, in practice an additional term proportional to the third-order derivative of $\mathbf{p}_c^{n+1}$ is introduced. Thus, in many aspects, this approach is similar to the popular Rhie and Chow (1983) interpolation method and eliminates checkerboard modes.

2.2 Large eddy simulation model

In LES, the largest, energy-carrying scales of the flow, are computed exactly, while the effect of the smallest scales of the turbulence are modelled by means of a subgrid-scale (SGS) model. The decomposition into a large-scale component and a small SGS is done by filtering spatially the Navier-Stokes equations (Eq. 1 and 2),

$$M\left(\overline{\mathbf{u}} - \overline{\mathbf{u}}_g\right) = \mathbf{0} \quad (5)$$

$$\frac{\partial \overline{\mathbf{u}}}{\partial t} + C\left(\overline{\mathbf{u}} - \overline{\mathbf{u}}_g\right)\overline{\mathbf{u}} + \nu D\overline{\mathbf{u}} + \rho^{-1}G\overline{\mathbf{p}} \approx -\mathrm{MT} \quad (6)$$

where $\overline{\mathbf{u}}$ and $\overline{\mathbf{u}}_g$ are the filtered velocities. The right term indicates some modelling of the non-linear convective term, in which *textM* is the divergence operator of a tensor and T the SGS stress tensor,

$$\mathrm{T} = -2\nu_{sgs}\overline{S} + (\mathrm{T} : I)I/3 \quad (7)$$

where $\overline{S} = \frac{1}{2}[G(\overline{\mathbf{u}}) + G^*(\overline{\mathbf{u}})]$, being G^* the transpose of the gradient operator. Then, the modelling is made through a suitable expression for the SGS viscosity, ν_{sgs}.

In this paper, LES have been performed using the wall-adapting local-eddy viscosity model (WALE) (Nicoud and Ducros (1999)), available in TermoFluids (Lehmkuhl et al. (2009, 2014)). This model is based on the square of the velocity gradient tensor. In its formulation, the SGS viscosity accounts for the effects of the strain and the rotation rate of the smallest resolved turbulent fluctuations. In addition, the proportionality of the eddy viscosity near walls ($\nu_{sgs} \propto y^3$) is recovered without any dynamic procedure,

$$\nu_{sgs} = (C_w\Delta)^2 \frac{(\mathrm{V}_{ij} : \mathrm{V}_{ij})^{\frac{3}{2}}}{(S_{ij} : S_{ij})^{\frac{5}{2}} + (\mathrm{V}_{ij} : \mathrm{V}_{ij})^{\frac{5}{4}}} \quad (8)$$

$$S_{ij} = \frac{1}{2}[G(\overline{\mathbf{u}}) + G^*(\overline{\mathbf{u}})] \quad (9)$$

$$\mathrm{V}_{ij} = \frac{1}{2}[G(\overline{\mathbf{u}})^2 + G^*(\overline{\mathbf{u}})^2] - \frac{1}{3}(G(\overline{\mathbf{u}})^2 I) \quad (10)$$

2.3 The Space Conservation Law

When dynamic meshes are used, the computational volume must be preserved, *i.e.* within a change of the position or the shape of a CV no space should be lost. This aspect is achieved by applying the so-called Space Conservation Law (SCL) (Orozco (2006); Breuer et al. (2012)):

$$\frac{d}{dt}\int_{\Omega(t)} d\Omega - \int_{S(t)} \mathbf{u}_g \cdot \mathbf{n}\, dS = 0 \quad (11)$$

where $\Omega(t)$ is a moving control volume bounded by a closed surface $S(t)$ of outward unit vector $\mathbf{n}$. The SCL allows to compute the unknown grid velocity avoiding the loss of mass and momentum. Actually, the mass conservation is automatically obtained by enforcing the SCL. However, the mass flux through a cell face c needs to be modified as follows (Shyy et al. (1996)):

$$\dot{m}_c^{modified} = \int_{S_c} \rho(\mathbf{u} - \mathbf{u}_g) \cdot \mathbf{n}\, dS \approx \rho_c(\mathbf{u} \cdot \mathbf{n})_c S_c - \rho_c\dot{\Omega}_c = \dot{m}_c - \rho_c\dot{\Omega}_c \quad (12)$$

$$\dot{\Omega}_c = (\mathbf{u}_g \cdot \mathbf{n})_c S_c = \frac{\delta\Omega_c}{\Delta t} \quad (13)$$

where $\delta\Omega_c$ represents the volume swept by the CV face c during the time step Δt. The volume swept is evaluated by an in-house conservative method, *i.e.* it is calculated exactly in order to consistently determine the additional grid fluxes in the momentum equation.

2.4 Grid adaptation

In fluid-structure interaction problems the motion of the structure is instigated by the fluid flow and viceversa, the flow field behaviour is affected by the movement or deformation of the structure. Therefore, the task is to dynamically adapt the inner computational mesh by transferring the predicted displacements at the interface with the structure to the inner grid points. In this study the grid adjustment is performed based on the RBF method, which is briefly described in this section. For further details the reader is referred to Boer et al. (2007); Jakobsson and Amoignon (2007); Estruch et al. (2012, 2013).

Let $\Omega \subset \mathbb{R}^d$ be the deformable domain, with $2 \le d \le 3$. We define $V = \{x_k\}_{k\in \Upsilon}$ as the vertices of the CFD grid covering Ω, where $\Upsilon = \{1, \cdots, N_v\}$ is the set of indexes and $|\Upsilon| = N_v$ the total number of vertices. The subset of pairwise vertices of the moving boundary, also called control points, is denoted by $V_b = \{\mathbf{x}_i\}_{i\in\Upsilon_b} \subset \Omega$, where $\Upsilon_b \subset \Upsilon$ and $|\Upsilon_b| = N_{v_b}$. Then, the following interpolation problem is considered: find a function $s^* \in T = \{s : \mathbb{R}^d \to \mathbb{R}\}, \ * \in \{x, y, z\}$ so that

$$s^*(\mathbf{x}) = \sum_{i\in\Upsilon_b} \gamma_i^* \varphi\left(\| \mathbf{x} - \mathbf{x}_i \|\right) \tag{14}$$

$$s^*(\mathbf{x}_i) = g_i^* \qquad \forall i \in \Upsilon_b \tag{15}$$

where $\gamma_i^* \in \mathbb{R}$ are the interpolation coefficients and $\mathbf{g}^* = \{g_i^*\}_{i\in\Upsilon_b}$ the known boundary displacements. This leads to the linear system of equations

$$\mathbf{M}\gamma^* = \mathbf{g}^* \tag{16}$$

where $\mathbf{M}$ is the interpolation matrix of dimension $N_{v_b} \times N_{v_b}$ containing the evaluation of the basis function $M_{ij} = \varphi(\| \mathbf{x}_i - \mathbf{x}_j \|)$.

The RBF adopted in this study is the Wendland C^2 (Eq. 17), which is of compact support and strictly definite positive (a support radius r is used to scale the compact support). Consequently, the interpolation matrix M is invertible, symmetric and strictly positive definite, and the linear system of equations can be solved by means of a conjugated gradient method (Saad (2003)).

$$\varphi(\mathbf{x}) \equiv \Phi\left(\frac{\| \mathbf{x} \|}{r}\right) = \Phi(\xi) = \begin{cases} f(\xi) = (1-\xi)^4(4\xi+1) & \text{if } \xi \in [0,1] \\ 0 & \text{otherwise} \end{cases} \tag{17}$$

3. VALVE DYNAMICS

As a first approach we consider a simplified geometry of an axial hole plus a rectangular diffuser (see Figure 2). In the context of compressor valves, the diffuser is considered like a flexible reed valve. Then, referring to Soedel (1992), the dynamic action of the valve is based on a specific law according modal analysis of valve reed theory. This methodology assumes that the valve motion results from the superposition of the valve vibration modes. In the following, the equations to solve the dynamics of the plate type reed valve are described.

According to the theory of vibrating systems (Thomson (1993); Soedel (1992)), the equation of motion of a reed type structure subjected to forced vibration is, in cartesian coordinates:

$$D\nabla^4 w(x,y,t) + \rho h \ddot{w}(x,y,t) = f(x,y,t) \tag{18}$$

where $\nabla^4 = \frac{\partial^4}{\partial x^4} + 2\frac{\partial^4}{\partial x^2 \partial y^2} + \frac{\partial^4}{\partial y^4}$, h the thickness of the structure, $f(x,y,t)$ the load per unit area at location (x,y) at time t and $D = \frac{Eh^3}{12(1-\nu^2)}$ the flexural rigidity of the structure, where E is the Young's modulus and ν the Poisson's ratio.

The numerical solution of Eq. 18 can imply considerable effort in time and cost. Therefore, the normal mode summation method (Thomson (1993)) is applied. Essentially, the displacement of the structure under forced excitation is approximated by a lineal combination of the normal modes of the system $\varphi_m(x,y)$ and generalized coordinates $q_m(t)$ (Eq. 19). For practical applications only the first few modes do actually participate and, consequently, only a finite number of normal modes are computed (typically, $m \le 3$).

$$w(x,y,t) = \sum_{m=1}^{\infty} q_m(t)\varphi_m(x,y) \tag{19}$$

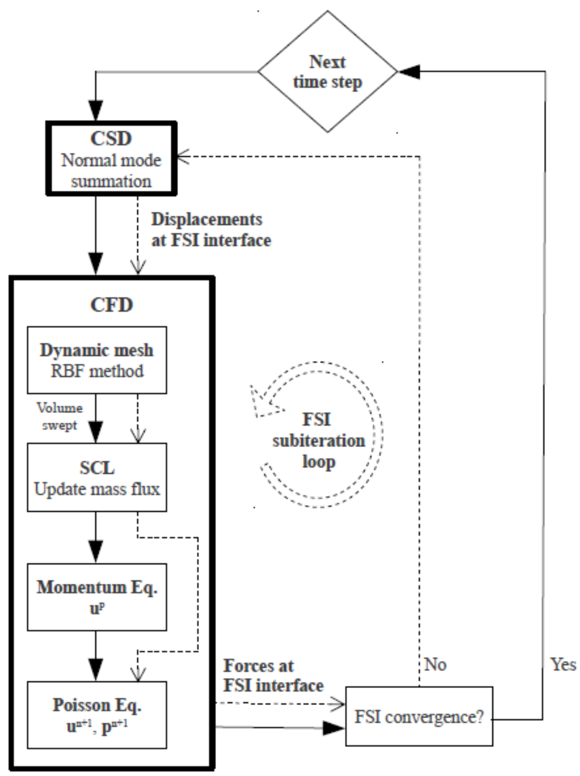

Figure 1: Partitioned strong FSI coupling scheme.

The normal modes $\varphi_m(x, y)$ and the respective normal natural frequencies ω_m can be evaluated analytically for simple cases; otherwise, for complicated configurations they should be evaluated experimentally. In this work the modal behaviour of the valve is supposed to be the same of a uniform cantilever beam; particularly, the normal modes of uniform beams have been tabulated by Young and Felgar (1949).

After some effort (Soedel (1992)) it leads to the following generalized equation, considering a valve reed of arbitrary geometry with k port holes:

$$\ddot{q}_m^{(t)} + 2\xi\omega_m\dot{q}_m^{(t)} + \omega_m^2 q_m^{(t)} = \frac{\Delta p(t)\sum_{i=1}^{k}\varphi_m(x_i, y_i)A_F(w(x_i, y_i))\Delta A_i}{A\rho h\sum_{j=1}^{l}\varphi_m^2(x_j, y_j)\Delta A_j} \tag{20}$$

where $\xi = \frac{c}{2m\omega_0}$ is the damping ratio, being c the damping coefficient and m the valve mass;$\Delta p(t)$ the pressure differential accross the valve; ΔA_i the area of the port hole at location (x_i, y_i); A the total port area; ΔA_j the area of the geometric discretization elements of the valve reed. The effective force area $A_F(w(x, y))$ is extracted from the analytical method presented in Schwarzler and Hamilton (1972). An implicit Crank Nicolson method is employed to integrate Equation 18.

In order to assure that the valve is not driven into its seat the following condition must be imposed:

$$w(x, y, t) \geq 0 \tag{21}$$

Moreover, the impact between the valve and its seat is assumed to occur in such a short period of time that only the velocity is affected by the collision. Hence, a coefficient of restitution C_r has been advocated in order to model the impact (Soedel (1992); Sheu and Hu (2000)). When the coefficient of restitution is set to zero, all the kinetic energy of the valve is changed into heat energy during impact.

$$\dot{q}_{\text{after impact}} = -C_r\dot{q}_{\text{before impact}} \tag{22}$$

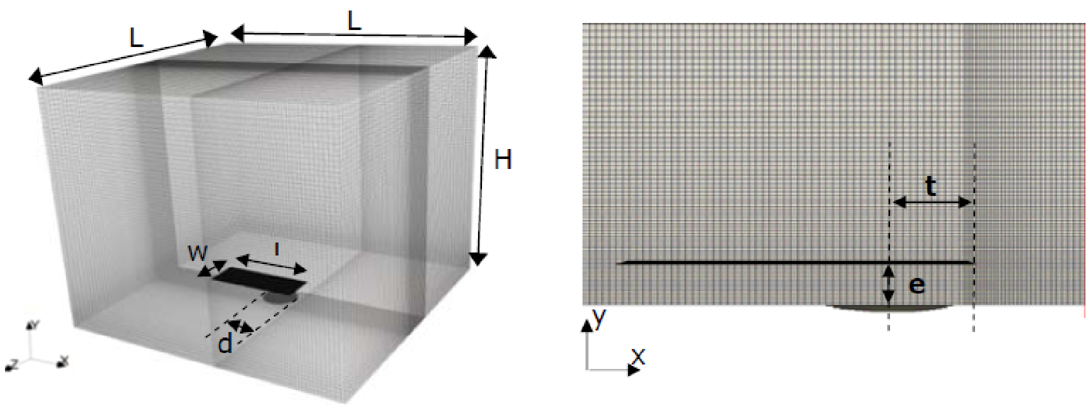

Figure 2: Computational mesh and domain. General view (left); zoom view (right).

4. FLUID-STRUCTURE COUPLING ALGORITHM

When dealing with FSI problems two essential modules are studied: the fluid solver and the structure solver, referring to the fluid solver as the CFD algorithm coupled with a dynamic mesh procedure. Coupling the fluid and structure domains and synchronizing them represents a big challenge (Farhat and Lesoinne (2000); Loon et al. (2006); Breuer et al. (2012)). The basic alternatives are: i) obtaining a simultaneous solution using monolithic schemes (Loon et al. (2006)), or ii) using a partitioned algorithm (Slone et al. (2002); Lv et al. (2007); Breuer et al. (2012)). The present study is focused on the latter, because of its stronger universality allowing to exchange codes for each subtask.

The strong FSI coupling scheme outlined in Figure 1 has been implemented, in which the solution of both subproblems are repeated in a staggered manner until a FSI convergence criterion is satisfied. However, for the present case the loose coupling approach is applied, what means that the fluid and the structure subproblem are only solved once per time step, *i.e.* without performing the FSI subiteration loop. This methodology is accepted for low density ratios of the fluid to the structure $\rho_f/\rho_s \ll 1$ or, equivalently, in case of a low so-called added mass effect (Causin et al. (2005)). Otherwise, for moderate or high density ratios stability problems could be encountered with a loose coupling procedure. Hence, for strong added-mass effect the strong coupling should be employed (Breuer et al. (2012)).

5. DEFINITION OF THE CASE

Figure 2 illustrates the computational mesh and domain containing the rectangular reed type valve. In the figure the inlet port hole of the valve is pointed out, which is centred at the bottom base and its diameter is d. The dimensions of the global domain are $L = 8.21d$ and $H = 6.15d$. The valve dimensions are: length $l = 2.70d$, width $w = 1.03d$ and thickness $h = 0.02d$. The height of the axial hole is $e = 0.37d$. In the initial configuration the valve is completely closed, *i.e.* is contained in the plane $y = e$, and it is translated $t = 0.62d$ in the x direction. The computational mesh is structured and has over 2.5 million CVs.

The fluid properties are: flow density $\rho_{fluid} = 7kg/m^3$ and dynamic viscosity $\mu_{fluid} = 8.3 \cdot 10^{-6} Pa\ s$. The valve material properties are: damping coefficient $c = 0.05N\ m/s$, material density $\rho_{valve} = 7870kg/m^3$, Young's modulus $E = 210 \cdot 10^9 Pa$. Notice that $\frac{\rho_{fluid}}{\rho_{valve}} = 8.9 \cdot 10^{-4} \ll 1$.

For the bottom inlet orifice a piston based inlet condition is assumed (see Figure 3), which is defined with a frequency of $50Hz$. A pressure based boundary condition applies for the outlet fluid exit (lateral and top walls). Non-slip boundary conditions are considered on solid walls (bottom part and valve reed). An immersed body procedure is used to simulate solid parts inside the domain and, hence, to reproduce the inlet and bottom boundaries (see Figure 4). Therefore, the RBF method allows the simulation from null valve deformation.

All computations have been performed on a cluster with 128 nodes, where each node has 2 AMD Opteron Quad-Core processors, and with 40 nodes, where each node has 32 Cores. The nodes are linked by means of an infiniband DDR4X network with latencies of 2.25 microseconds with 20Gbits/s bandwidth.

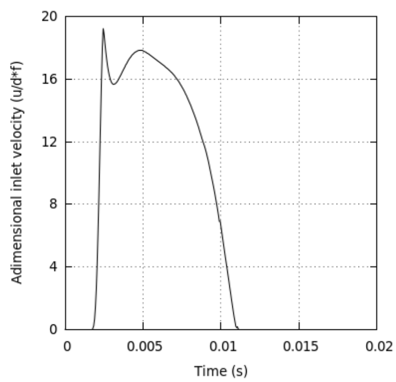

Figure 3: Piston based inlet boundary condition.

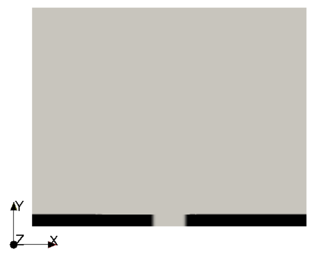

Figure 4: Immersed boundary procedure. Solid: black; fluid: grey.

6. NUMERICAL RESULTS

The results presented in this section pretend to be a preliminary illustrative study of the transient and dynamic simulation of the fluid flow through a suction reed valve subjected to a piston based inlet boundary condition and considering a modal model for the valve dynamics.

The flow phenomena observed is consistent with previous studies (Rigola et al. (2008, 2009, 2012)) and accomplishes a qualitative accurate transient simulation of the turbulent flow through the valve reed. For instance, the velocity and pressure profiles for different states during the suction process are shown in Figures 5 and 6. In agreement with the sudden increment of the inlet velocity according to the piston based inlet boundary condition (Figure 3), a considerable increase of velocity is appreciated in the valve reed aperture when it starts to open. Hence, huge velocity gradients and consequently high vorticity appear in this area, where the mesh should be particularly fine to capture the smallest scales of the flow. Referring to this, the RBF method allows that the mesh quality is maintained in this region, provided that the initial mesh has sufficient number of CVs below the valve plate and the parameter radius of the RBF interpolation is chosen appropriately. Therefore, the CFD and dynamic mesh coupled code TermoFluids would be capable to carry out successfully the transient simulation of the flow through the reed valve, even with more complex geometries.

A parametric analysis is presented in Figure 7, in which the motion of the hole centre point is depicted for different valve thickness values. The numerical results show that the dynamic action of the reed valve is definitely dependent on this parameter, leading to larger deflections when the thickness is smaller. Moreover, for higher thickness values the reed valve tends to oscillate with a greater frequency during the opening cycle, implying a major number of impacts between the valve and its seat, what in practice can influence to structural or acoustic issues.

7. CONCLUSIONS

The transient numerical simulation of the fluid flow through a suction reed valve has been carried out using the in-house implemented partitioned loose FSI coupling scheme, based on the CFD code TermoFluids with dynamic grid adaptation through the RBF interpolation procedure. The valve dynamic action has been modelled as a flexible reed valve by means of the normal mode summation strategy. As a first approach a simplified geometry of an axial hole

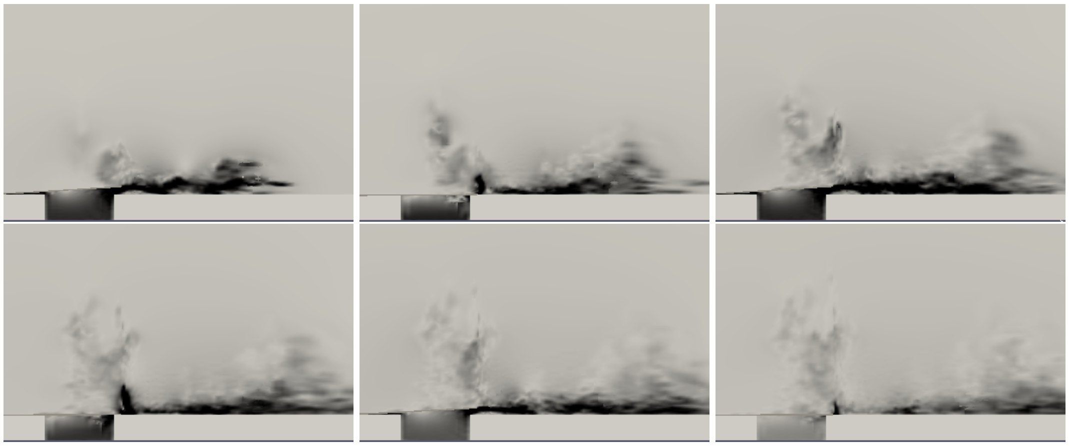

Figure 5: Velocity profiles during the suction process.

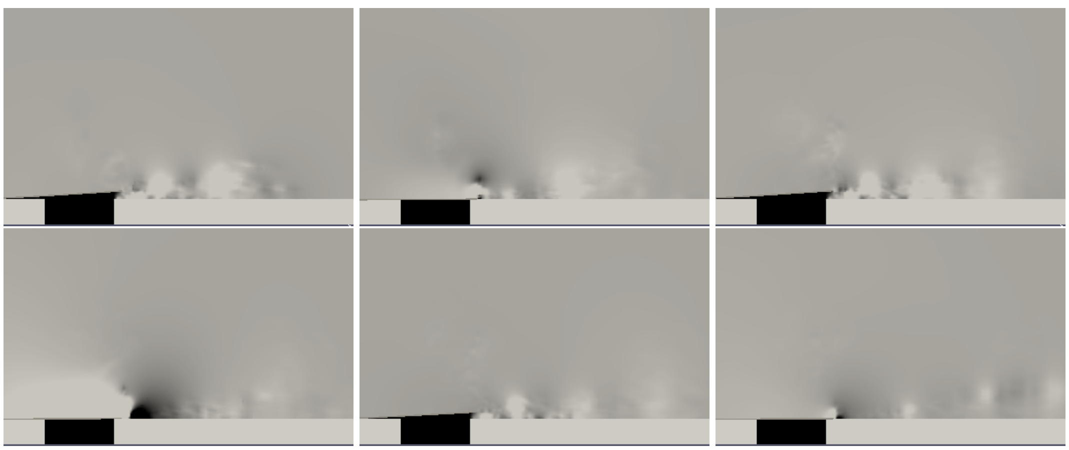

Figure 6: Pressure profiles during the suction process.

plus a rectangular reed valve has been analysed. The algorithm has been capable to reproduce the cycle of movement capturing the turbulent flow phenomena with qualitative precision, even with a relatively coarse mesh. A parametric analysis based on the valve thickness has been performed, demonstrating that the choice of this parameter is a crucial aspect for the design of reed valves, since it could be involved in structural an acustic problems related with the collisions between the valve and its seat.

We consider to extrapolate the study to other more complex geometries of the reed valve and to contrast the structural results to a higher level CSD solver.

NOMENCLATURE

$\mathbf{u}$	velocity vector	D	diffusive operator
$\mathbf{p}$	pressure	t	time
$\mathbf{u}_g$	surface velocity vector	φ	radial basis function
ν	kinematic viscosity	$\|\cdot\|$	Euclidean norm
ρ	density	$w(x,y,t)$	transverse deflection
M	divergence operator	$\varphi_m(x,y)$	m^{th} normal mode shape function
G	gradient operator	ω_m	m^{th} normal natural frequency
C	convective operator	$A_F(w(x,y))$	effective force area

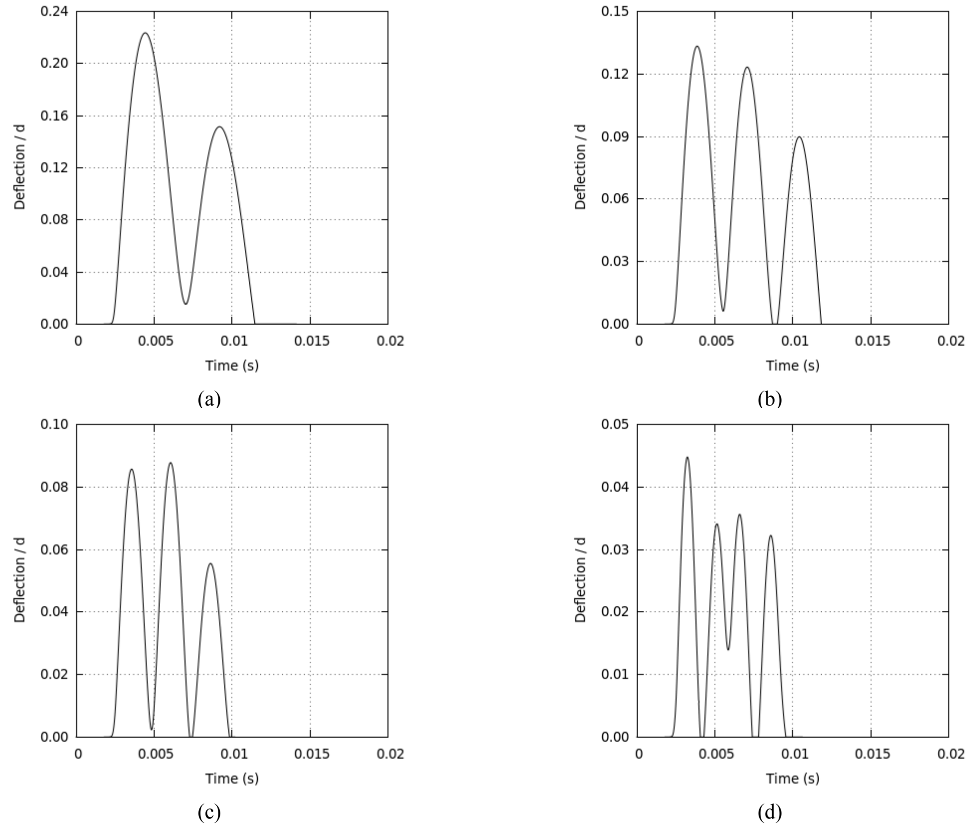

Figure 7: Hole centre motion for different valve thickness values: (7a) $0.5h$**; (7b)** $0.75h$**; (7c)** h**; (7d)** $1.5h$**.**

REFERENCES

Boer, A. D., der Schoot, M. V., and Bijl, H. (2007). Mesh deformation based on radial basis function interpolation. *Comp. and Struct.*, 85:784--795.

Breuer, M., Nayer, G. D., Münsch, M., Gallinger, T., and Wüchner, R. (2012). Fluid-structure interaction using a partitioned semi-implicit predictor-corrector coupling scheme for the application of large-eddy simulation. *J. of Fluids and Struct.*, 29:107--130.

Causin, P., Gerbeau, J., and Nobile, F. (2005). Added-mass effect in the design of partitioned algorithms for fluid-structure problems. *Comp. Meth. in App. Mech. and Eng.*, 194:42--44.

Estruch, O., Lehmkuhl, O., Borrell, R., and Pérez-Segarra, C. (2012). Large-eddy simulation of turbulent dynamics fluid-structure interaction. In *Proc. of the 7th Int. Synopsium on Turbulence, Heat and Mass Transfer*, Palermo.

Estruch, O., Lehmkuhl, O., Borrell, R., Pérez-Segarra, C., and Oliva, A. (2013). A parallel radial basis function interpolation method for unstructured dynamics meshes. *Comp. and Fluids*, 80:44--54.

Farhat, C. and Lesoinne, M. (2000). Two efficient staggered algorithms for the serial and parallel solution of three-dimensional nonlinear transient aerolastic problems. *Comp. Meth. in App. Mech. and Eng.*, 182:499--515.

Jakobsson, S. and Amoignon, O. (2007). Mesh deformation based on radial basis function interpolation. *Comp. and Fluids*, 36:1119--1136.

Lehmkuhl, O., Calafell, J., Rodríguez, I., and Oliva, A. (2014). Large-eddy simulations of wind turbine dedicated airfoils at high reynolds numbers. In *Wind Energy - Impact of Turbulence*, volume 2, pages 147--152.

Lehmkuhl, O., Perez-Segarra, C., Borrell, R., Soria, M., and Oliva, A. (2009). Termofluids: A new parallel unstructured cfd code for the simulation of turbulent industrial problems on low cost pc cluster. In *Parallel CFD 2007*, volume 67, pages 275--282.

Loon, R. V., Anderson, P., and van de Vosse, F. (2006). A fluid-structure interaction method with solid-rigid contact for heart valve dynamics. *J. Comp. Physics*, 217:806--823.

Lv, X., Zhao, Y., Huang, X., Xia, G., and Su, X. (2007). A matrix-free implicit unstructured multigrid finite volume method for simulating structural dynamics and fluid-structure interaction. *J. Comp. Physics*, 225:120--144.

Nicoud, F. and Ducros, F. (1999). Subgrid-scale stress modelling based on the square of the velocity gradient tensor. *Flow, Turbulence and Combustion*, 62:198--200.

Ooi, K., Chai, G., and Kwek, E. (1992). A simple valve model to study the performance of a small compressor. In *Int. Comp. Eng. Conf.*, Paper 803.

Orozco, C. (2006). *Finite volume computation and verification of fluid flow and heat transfer phenomena in domains with moving boundaries and complex geometries*. ETSEIT (UPC).

Rhie, C. and Chow, W. (1983). Numerical study of the turbulent flow past an airfoil with trailing edge separation. *AIAA Journal*, 21:1525--1532.

Rigola, J., Lehmkuhl, O., Oliva, A., and Pérez-Segarra, C. (2009). Numerical simulation of the fluid flow through valves based on large eddy simulation models. In *Int. Conf. on Comp. and their Systems*, pages 137--145, London.

Rigola, J., Lehmkuhl, O., Pérez-Segarra, C., and Oliva, A. (2008). Numerical simulation of the fluid flow through valves reeds based on large eddy simulation models (les). In *Int. Comp. Eng. Conf.*

Rigola, J., Lehmkuhl, O., Ventosa, J., Pérez-Segarra, C., and Oliva, A. (2012). Numerical simulation of the turbulent fluid flow through valves based on low mach models. In *Int. Comp. Eng. Conf.*

Saad, Y. (2003). *Iterative Methods for Sparse Linear Systems*. Society for Industrial and Applied Mathematic, 2nd edition.

Schwarzler, D. and Hamilton, J. (1972). An analytical method for determining effective flow and force areas for refrigerating compressor valving system. In *Int. Comp. Eng. Conf. at Purdue University, IIF/IIR*, pages 30--36.

Sheu, H. and Hu, Y. (2000). Nonlinear vibration analysis of reed valves. In *Int. Comp. Eng. Conf.*, Paper 1419.

Shyy, W., Udaykumar, H. S., Rao, M. M., and Smith, R. W. (1996). *Computational fluid dynamics with moving boundaries*. Taylor and Francis.

Slone, A., Pericleous, K., Bailey, C., and Cross, M. (2002). Dynamic fluid-structure interaction using finite volume unstructured mesh procedures. *Comp. and Struct.*, 80:371--390.

Soedel, W. (1992). *Mechanics, simulation and design of compressor valves, gas passages and pulsation mufflers*. Purdue University Short Courses, IN, USA.

Thomson, W. (1993). *Theory of Vibration With Applications*. Prentice-Hall, Inc., Englewood Cliffs, 4th edition.

Trias, F. and Lehmkuhl, O. (2011). A self-adaptive strategy for the time integration of navier-stokes equations. *Numerical Heat Transfer, Part B: Fundamentals*, 60:116--134.

Verstappen, R. and Veldman, A. (2003). Symetry-preserving discretization of turbulent flow. *J. of Comp. Physics*, 187:343--368.

Young, D. and Felgar, R. (1949). *Tables of characteristics functions representing normal modes of vibration of a beam*. The University of Texas Publication No. 4913.

ACKNOWLEDGEMENT

This work has been financially supported by the Ministerio de Educación y Ciencia, Secretaría de Estado de Universidades e Investigación, Spain (ref. ENE2010-17801) and by the Collaboration Project between Universitat Politècnica de Catalunya and TermoFluids S.L. (ref. C06650).